

## Magneto-optical microscopy and its application

Rudolf Schäfer

IFW Dresden, Inst. f. Metallic Materials,  
Helmholtzstr. 20, D-01069 Dresden  
r.schaefer@ifw-dresden.de

The magnetic microstructure, i.e. the arrangement of domains and domain walls, forms the mesoscopic link between basic physical properties of a magnetic material and its macroscopic properties. Hysteresis phenomena, energy loss in inductive devices, noise in sensors, or the magnetoresistive properties of modern spintronic devices are decisively determined by the peculiarities of the underlying magnetic microstructure, especially by irreversibilities in the magnetization process. The development and optimization of magnetic materials therefore requires a solid knowledge of the underlying domains and their reaction to magnetic fields. In most cases, such knowledge can only be gleaned by direct imaging.

Although there has been considerable progress in magnetic imaging in recent years, culminating in the development of a variety of nanoscale imaging techniques, several technical assets inherent to the classical Kerr technique make it arguably the most versatile and flexible imaging technique. Kerr microscopy exploits the magneto-optical Kerr effect, i.e. the magnetization-dependent rotation of plane-polarized light upon reflection from a non-transparent magnetic sample (Fig. 1). By means of an analyser in an optical reflection polarization microscope this rotation is converted into a (in general weak) domain contrast that can be enhanced by digital image processing. When used in conjunction with an image processor, Kerr microscopy can extract domain contrast from the surface of virtually any ferro- or ferrimagnetic sample. Often no specific surface treatment is required and even some coatings may be allowed. The basic components of a Kerr-setup are shown in Fig. 2.

Magnetic fields of arbitrary strength and direction can be applied to the sample, making it possible to observe magnetization processes and to simultaneously measure the localized magnetization loops, governing those processes (Fig. 3). Magnetization dynamics can be studied at arbitrary frequencies, spanning the entire range between slow processes (as fast as the eye can follow), to excitations beyond the Giga-Hertz regime by employing time-resolved, stroboscopic imaging methods – see Figs. 4 and 5. An example of such a high-speed experiment is presented in Fig. 6.

Samples may be heated and cooled in optical heating stages and cryostats, respectively, so that magnetic phase transitions or other thermal effects on the magnetic microstructure can be investigated. Mechanic sample deformation during domain observation is easily possible in a Kerr microscope, which makes the study of stress effects on domains possible. For low-anisotropy materials, the magnetization vector field on the sample surface can be quantitatively evaluated (Fig. 7). The information depth of Kerr microscopy is in the ten-nanometer regime for metallic materials, allowing the depth selective observation of

magnetization distributions in layered sample systems (Fig. 8) as they are currently developed and investigated for spintronic applications. Such multilayer structures can also very favorably be investigated by applying the depth sensitivity of the magneto-optical Voigt- and Gradient effect two other effects that become visible in an optical polarization microscope. The difference between the effects in comparison with the (most commonly used) Kerr effect is demonstrated in Fig. 9.

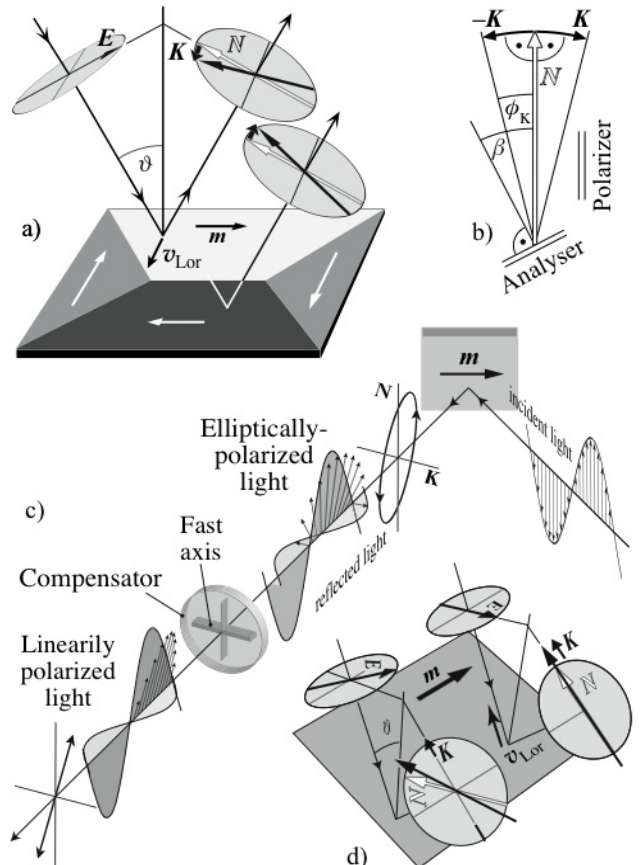


**Fig. 1** (a) Illustration of the elementary magneto-optical interaction for the longitudinal Kerr effect. The sample with in-plane magnetization is illuminated using light that is polarized parallel to the plane of incidence. The electric field vector  $E$  of the incident light, together with the magnetization vector  $\mathbf{m}$ , generates a Lorentz movement of the electrons (“right-hand rule”). If the resulting Lorentz speed  $v_{\text{Lor}}$  is then projected onto the plane perpendicular to the direction of propagation of the reflected light, the magneto-optical amplitude  $\mathbf{K}$  is obtained (a similar  $\mathbf{K}$ -component would also be generated if the light would be polarized perpendicular to the plane of incidence). The interference of the normally reflected component  $N$  and the Kerr component  $\mathbf{K}$  results in magnetization-dependent light rotation by a small angle  $\phi_K$ , which, by using an analyser, leads to the domain contrast (b). The analyser should actually be set at the angle  $\beta > \phi_K$  to optimize the domain visibility. A compensator (c) converts elliptical light into a linear wave by shifting the two constituent, orthogonal wave components. The symmetry of the transverse Kerr effect is explained in (d). Only light of parallel polarization yields an effect, so that a Kerr rotation is only possible at 45° polarization

Since the magnification is so easily varied by the mere changing of a microscope objective, the user can quickly go from overview observations in the centimeter regime, to detailed studies of samples with micrometer size. The lateral resolution of optical microscopy with visible light is limited to about 300 nm by the Raleigh

criterion. This can be a drawback for the study of sub-micrometer patterned structures or for certain micromagnetic objects like vortices or stripe domains in very thin films. But for the imaging of most features of magnetic microstructure the resolution is sufficient (Fig. 10). In bulk samples only the magnetization of the surface region can be seen, but this limitation applies to most other imaging techniques as well. Nevertheless, in many cases the volume domains can indirectly be seen or at least guest by surface observations in applied magnetic fields.

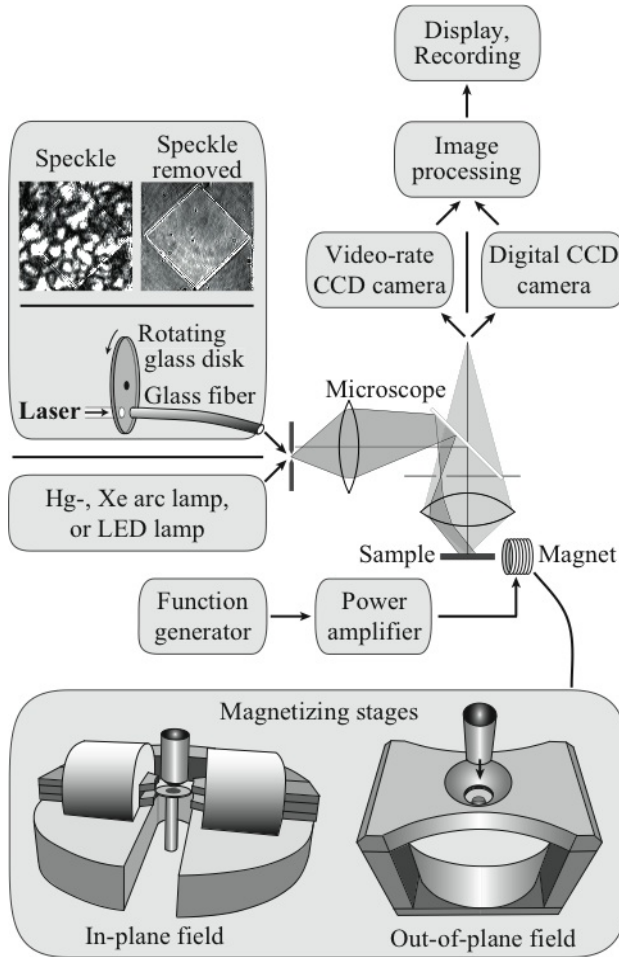


**Fig. 2** Experimental setup for wide-field Kerr microscopy. Options are shown for illumination, video processing and magnetizing stages. Also shown is the presence and suppression of interference patterns by laser illumination with and without rotating glass disk, respectively, on a 28 by 28  $\mu\text{m}^2$  Permalloy thin film element

There are rare cases of samples that do not provide sufficient Kerr contrast. An example is the NiMnGa magnetic shape memory alloy. Here polarization optics just reveals the crystalline microstructure. Domains can indirectly be imaged by applying indicator films on top of the surface (Fig. 11). Stray fields, emerging from the domains at the sample surface, induce a polar magnetization component in the active layer of the detector which is recorded by the polar Faraday effect.

Since the earliest applications of Kerr microscopy in 1951, continuous methodical developments have greatly enhanced the capabilities of the traditional Kerr technique. In this presentation we shall review the widespread capabilities of contemporary magneto-optical microscopy, as

well as the physical and technological fundamentals that underlie the method. Numerous images on a great variety of novel magnetic materials will be shown to demonstrate the advantages and special features of the technique. Comprehensive reviews on domain imaging with emphasis on magneto-optical microscopy are given in [1, 2] where also an extended bibliography can be found.

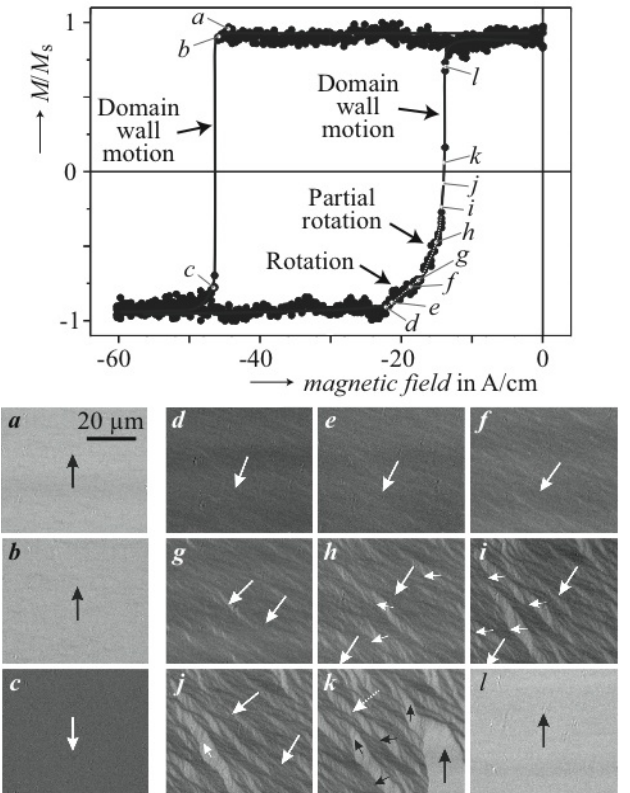


**Fig. 3** Magneto-optical hysteresis curve, directly measured in a wide-field Kerr microscope, together with domain images on a CoFe (20 nm)/IrMn (10 nm) bilayer film. Shown are the domains in the ferromagnetic CoFe film, which is exchange coupled to the antiferromagnetic IrMn film that is responsible for the loop shift (exchange bias effect). The steep forward branch of the magnetization curve is caused by domain wall motion (a – c), while inhomogeneous rotational processes (d – k) are responsible for the rounded part of the recoil branch. The wall motion along the forward branch is so fast that it cannot be recorded by static images. The magnetization  $M$  is normalized to the saturation magnetization  $M_s$  in the plot [courtesy J. McCord]

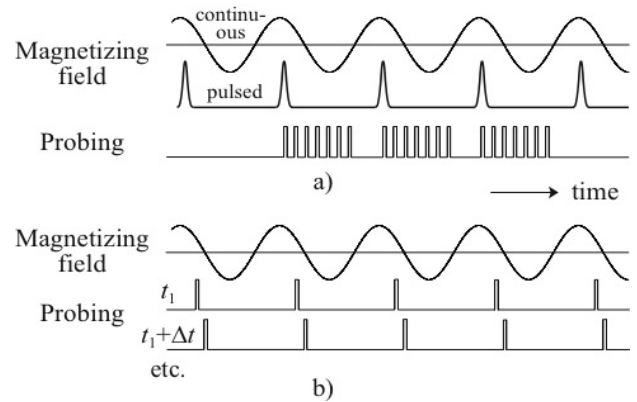


**Fig. 4** Principle of time resolved imaging, (a) for an ideal single-shot experiment, and (b) in the stroboscopic mode. The sample is excited either by alternating magnetic fields or a by train of field pulses

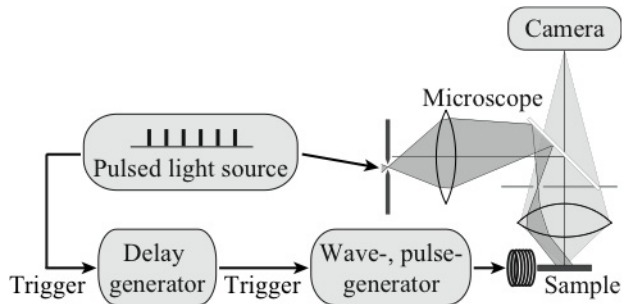


**Fig. 5** Block diagram for light-based stroboscopic wide-field microscopy. A pulsed light source is employed for time-resolution

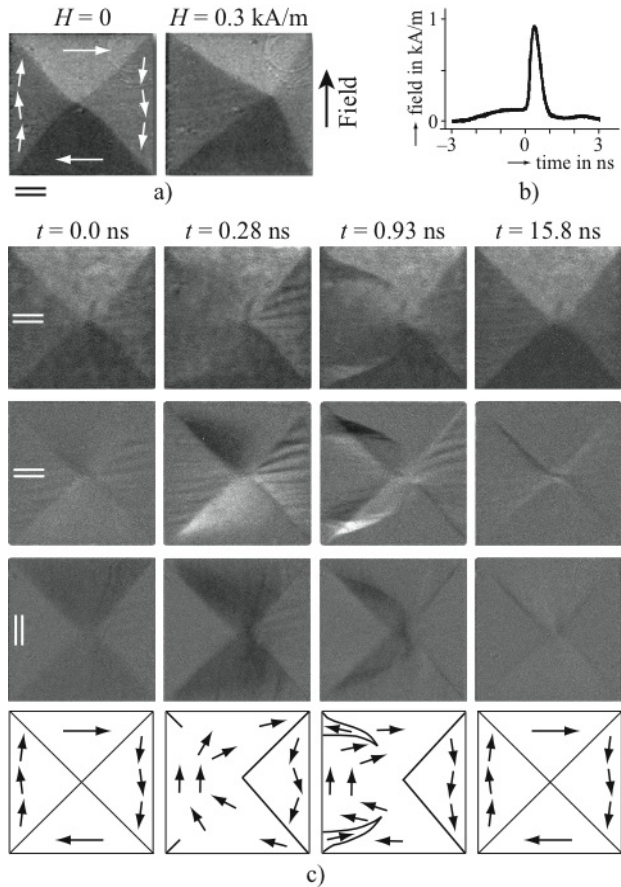


**Fig. 6** Excitation of a Landau ground state in a permalloy thin film element (edge length 40  $\mu\text{m}$ , thickness 50 nm) in magnetic fields parallel to the edge. (a) Quasistatic process. The dynamic process (c), excited by a sharp field pulse (b), is completely different. Shown are difference images: In the upper row of (c) an image of the saturated state was subtracted, while images of the Landau ground state were subtracted in the middle and lower row at different Kerr sensitivity directions as indicated, highlighting changes of the magnetization. Indicated are the time delays where the images have been captured in a stroboscopic way. The accumulation of some  $10^6$  single pictures, each of them obtained with a laser pulse of about 20 ps length, was necessary to obtain an image of sufficient contrast. [Together with A. Neudert and J. McCord]

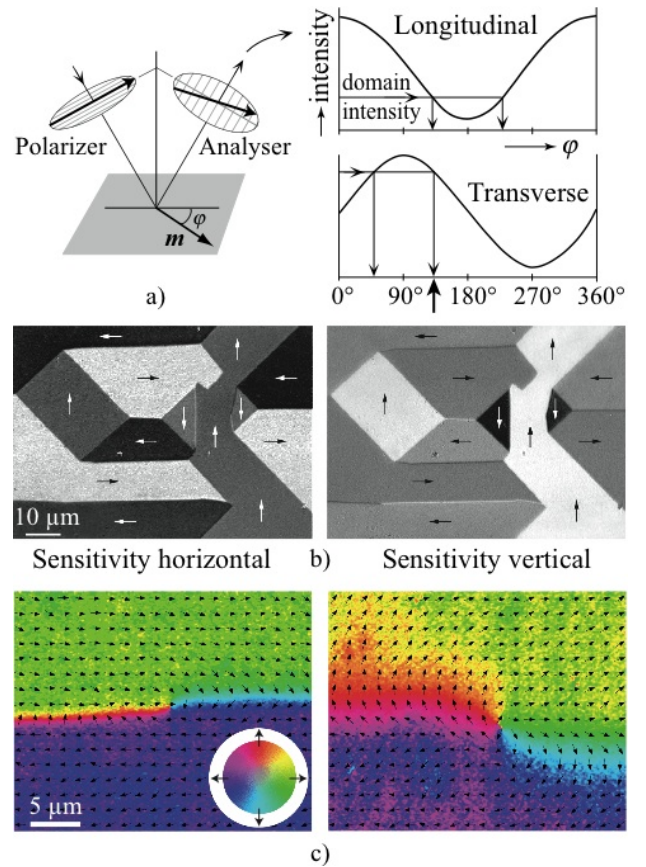


**Fig. 7** Principle and application of quantitative Kerr-microscopy. (a) Calibration functions of the Kerr intensity at longitudinal and transverse sensitivity as a function of magnetization direction (schematically). The intensities of an unknown domain, measured under the same conditions, are compared with the calibration functions as indicated by arrows. (b) Domain pattern on iron-silicon [100] sheet, imaged under two complementary Kerr-sensitivities. (c) Quantitative images on a Co-rich amorphous ribbon. The domain wall width of the as-quenched state (left) is strongly enlarged (right) if residual anisotropies are reduced by annealing in a rotating magnetic field. A vector plot and color code can be used for presentation

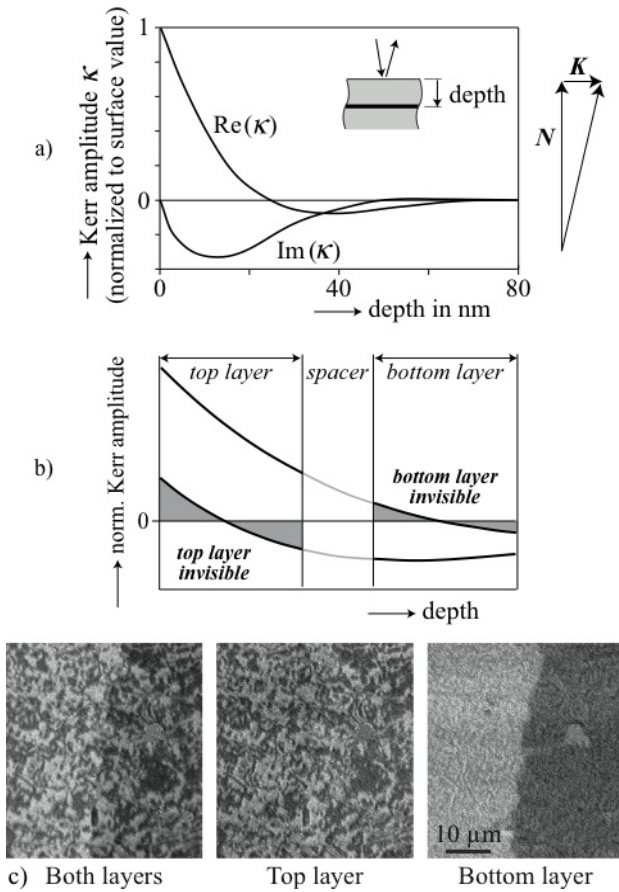


**Fig. 8** (a) Depth-sensitivity of the normalized Kerr amplitude  $\kappa$  in iron. The relative phase of  $\mathbf{K}$  and  $\mathbf{N}$  was selected so that  $\mathbf{N}$  is allowed to interfere with the  $\mathbf{K}$  generated right at the surface. Proper phase selection (b – schematically) allows layer-selective Kerr imaging on thin-film sandwiches as demonstrated in (c) for a sputtered Co/Cu/Ni<sub>8</sub>Fe<sub>19</sub> (5 nm/ 5 nm/ 50 nm) tri-layer. [imaging courtesy J. McCord, IFW Dresden]

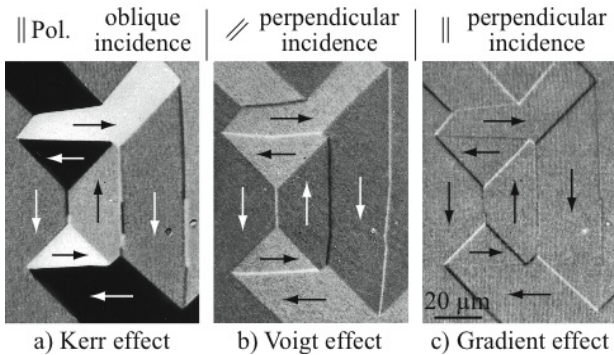


**Fig. 9** Domains on a (100) surface of silicon-iron (Fe 3 wt% Si, sheet thickness 0.3 mm), imaged in the magneto-optical Kerr-(a), Voigt-(b) and Gradient-effect (c). The Kerr effect is linear in the magnetization vector, so the four domain phases in (a) show up in different colors. The same pattern imaged in the Voigt effect displays only two colors, one for each magnetization axis. This contrast is independent of the magnetization direction since the Voigt effect depends quadratically on the magnetization vector. The Gradient effect is sensitive to changes in magnetization. Therefore domain boundaries show up in this effect with a contrast depending on the relative magnetization directions of the neighboring domains. Both, Voigt and Gradient effect are strongest at perpendicular incidence of light and require a compensator for contrast adjustment.

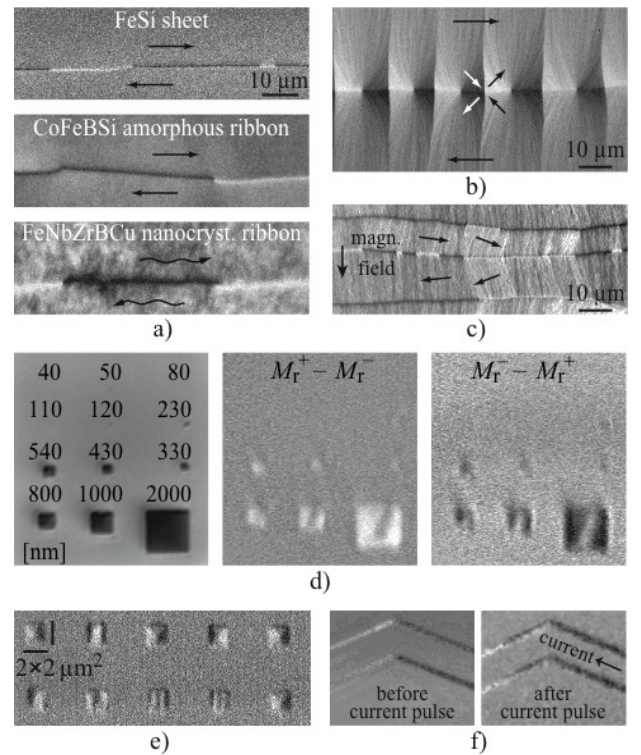


**Fig. 10** High-resolution Kerr observations. (a) Domain wall imaging on different bulk samples. The surface wall width for the FeSi Goss sheet (300 nm thick) with (110) surface orientation is 150 nm, for the metallic glass (25 μm thick) it is 0.9 μm, and for the nanocrystalline ribbon (20 μm thick) a surface wall width of 1.6 μm is measured, as expected due to the decreasing anisotropy in the order of materials. The black-white contrast of the wall segments is caused by the rotation sense of magnetization (see also Figure 4a). (b) Cross-tie wall in a 40 nm thick Permalloy film, and (c) coexisting asymmetric Bloch- and Néelwalls in a 460 nm thick Permalloy film, the latter being characterized by a double-contrast. See ref. [1] for details. (d) Regular image (left) and difference images between the remanent states after positive and negative saturation (middle) and vice versa (right) on quadratic cobalt elements of various sizes. The saturation field was aligned vertically, indicated is the edge length of the elements in nanometer. (e) Domain patterns in an array of 2 μm wide Co elements after ac-demagnetization. In (f) the head-on domain walls in 500 nm wide NiFe stripes were shifted by current pulse injection. [(f) together with J. McCord and M. Kläui]

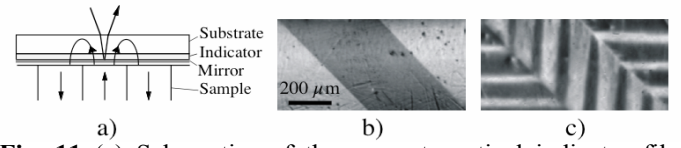


**Fig. 11** (a) Schematics of the magneto-optical indicator film technique and application to a NiMnGa magnetic shape memory alloy: (b) structural contrast, showing two twin variants, (c) domain contrast, obtained by an indicator film on top of the surface [courtesy Y. Lai and J. McCord]

## Bibliography

- [1] A. Hubert and R. Schäfer: Magnetic Domains. The Analysis of Magnetic Microstructures. Springer Verlag, Berlin (1998)
- [2] R. Schäfer: Investigation of domains and dynamics of domain walls by the magneto-optical Kerr effect. In Handbook of Magnetism and Advanced Magnetic Materials. ed. by H. Kronmüller and S. Parkin, Wiley (2007)